Title: Direct Detection of a BRAF Mutation in total RNA from Melanoma Cells

Authors:

F. Huber[a], H. P. Lang[a], N. Backmann[a], D. Rimoldi[b,c] and Ch. Gerber[a,c]

a Swiss Nano Institute, University of Basel, Klingelbergstrasse 82, 4056 Basel, Switzerland

b Ludwig Center for Cancer Research of the University of Lausanne, 1066 Epalinges, Switzerland

c these authors equally contributed to this work

Malignant melanoma, the deadliest form of skin cancer, is characterised by a predominant mutation in the BRAF gene. Drugs that target tumours carrying this mutation have recently entered the clinic. Therefore patients are routinely screened for mutations in this gene to determine whether they can benefit from this type of treatment. The current gold standard for mutation screening uses real time polymerase chain reaction (PCR) and sequencing methods. Here we show that an assay based on microcantilever arrays can detect the mutation nanomechanically without amplification in total RNA samples isolated from melanoma cells. The assay is based on a BRAF specific oligonucleotide probe. We detected mutant BRAF at a concentration of 500 pM in a 50-fold excess of the wild-type sequence. The method was able to distinguish melanoma cells carrying the mutation from wild type cells using as little as 20 ng/µl of RNA material, without prior PCR amplification and use of labels.

The identification of alterations in specific signalling pathways and recurrent oncogenic mutations in particular types of cancers has led in the past decade to the explosion of targeted therapy approaches. In cutaneous melanoma, a significant improvement in overall survival has been achieved by vemurafenib and similar drugs that selectively inhibit tumours carrying a mutated *BRAF*

gene[1,2]. Additional drugs for combination therapies with higher efficacies and fewer side effects are in clinical trials[3]. *BRAF* is one of three *RAF* genes (rapidly accelerated fibrosarcoma A, B and C) encoding cytoplasmic protein serine/threonine kinases belonging to the mitogen-activated protein kinase (MAPK) signal transduction cascade, a pathway controlling various cellular processes such as proliferation, migration and survival[4,5]. *BRAF* somatic mutations are present in half of cutaneous melanomas. Over 90% of the mutations are a single T to A transversion at position 1799 in the BRAF coding sequence (cT1799A), which converts a valine amino acid residue at position 600 in the protein to a glutamic acid (V600E). This mutation renders the protein constitutively active, resulting in a deregulated MAPK pathway[6] and thus uncontrolled cell growth and cancer. BRAF mutations are also present in other neoplasms, including hairy cell leukemias, thyroid and colon carcinomas[7,8,9]. As the presence of the cT1799A/V600E BRAF (hereafter $BRAF^{V600E}$) mutation determines eligibility to BRAF inhibitor treatment, molecular screening of tumour biopsies is now carried out routinely. Various methods have been developed for the detection of the $BRAF^{V600E}$ mutation at the DNA level. Among them is the long established procedure of PCR amplification coupled with Sanger sequencing of the product. The standard test currently employed to analyze patients' biopsies before initiation of vemurafenib treatment relies on real time PCR (the COBAS™ Test[10]), whereby 5-10% of BRAF-mutated melanoma cells can be detected in a background of normal cells. Alternative technologies to classic methods are under development, such as cycling temperature capillary electrophoresis[11] with sensitivity comparable to COBAS™, silicon nanowire field-effect transistors[12] and a three-dimensional gold nanowire platform[13]. The latter technologies have only been shown to work using synthetic oligonucleotide targets, larger gene fragments or still rely on an initial PCR amplification. In particular, they have not been applied to the direct identification of a mutated messenger RNA (mRNA) sequence in total RNA (constituted primarily by ribosomal RNA and containing all mRNAs transcribed from genes) or DNA samples.

In recent years a versatile platform for biodetection has been developed based on microfabricated arrays of silicon cantilevers[14,15,16,17,18,19,20,21], each coated with a sensitive layer for molecular recognition, e.g. a gene specific oligonucleotide. The binding of the target sequence is mechanically transduced to the cantilever surface resulting in bending of the cantilever. Such devices represent ultrasensitive sensors for the detection of biochemical interactions in liquid environments[22]. Here we have explored the feasibility of applying this technology to discriminate between $BRAF^{V600E}$ and wild type BRAF sequences in melanoma samples.

In a first set of experiments aimed at assessing the specificity of detection of the $BRAF^{V600E}$ mutation with cantilever arrays we chose as a probe a surface-immobilized thiolated 13-mer oligonucleotide (V600E_short; see Table 1) carrying at the centre the mutated nucleotide (adenine instead of thymidine, labelled in red). The short length is sufficient to provide a unique sequence which is not present anywhere else in the BRAF PCR product and a central position of the mismatch was selected as it allows the highest discrimination between the wild type and the mutant sequence. To ensure a high surface density of the BRAF-specific probe layer, preliminary tests were performed to optimise the adsorption of V600E_short thiol oligonucleotide probes onto a gold-coated cantilever surface (Supplementary Figures 1 and 2). Based on the results obtained, we decided to use the highest concentration (40 µM), corresponding to over 90% occupancy[23], thus ensuring a large cantilever bending signal in all subsequent hybridization experiments. We also confirmed the reusability of the sensor by repeated injections of a 13-mer complementary oligonucleotide preceded by urea washing steps (Supplementary Figure 3).

We applied the array functionalized as shown in Fig. 1 to distinguish between a wild type and a mutated BRAF sequence. For these experiments, we utilised PCR amplified cDNA (complementary DNA derived from mRNA by reverse transcription) samples ($BRAF^{V600E}$ PCR, 621 bp long) derived from melanoma cells expressing either wild type BRAF or mutant $BRAF^{V600E}$. Fig. 2a shows the differential signals obtained after injection of pure wild type or mutated BRAF sequences, as well as

after injection of increasing dilutions (wild type to mutant from 1:1 to 50:1) of the mutated into the wild type sequence.

The cantilevers selectively responded to the mutated BRAF sequence and the amplitude of deflection scaled with the concentration of target DNA or RNA. Furthermore, the mutant gene sequence could still be detected in the presence of 50 fold excess of wild type DNA sample (i.e. when present at 2% level). In each experiment the total DNA concentration was kept constant at 10ng/µl DNA. As the size of the fragments used is 621 base pairs, corresponding to a molecular weight of $4x10^5$ Dalton, the results indicate a detection limit of approximately 500 pM $BRAF^{V600E}$ DNA in the presence of excess wild type sequence. Fig. 2b shows the Langmuir isotherm fitted to the equilibrium values of responses extracted from Fig. 2a, plotted against the concentration of $BRAF^{V600E}$ PCR product. The dG value of -49.8 $KJmol^{-1}$ calculated from the Langmuir plot is in good agreement with results previously reported for hybridization experiments with oligonucleotides of similar length using microcantilevers (dG = -41.4 $kJmol^{-1}$) [15] and surface plasmon resonance (SPR) data (dG = -43.4 $kJmol^{-1}$)[24] , as well as theoretical calculations in solution (dG = -50.5 $kJmol^{-1}$)[25]. The minor deviation of our measurement from these values can be explained by the double stranded nature and the length of the fragments analysed.

Messenger RNAs are present in cells at a higher copy number than the corresponding genes. In addition, RNA/DNA interactions are stronger than DNA/DNA interactions[26]. We thus directly detected the BRAF mutation at the RNA level without prior amplification steps (e.g. PCR). For that purpose we designed an oligonucleotide probe to unambiguously identify the mutated BRAF mRNA sequence. Based on the expressed sequence tags database of the human genome we determined a minimum required length of 18 bases to specifically detect BRAF mRNA. As total RNA is a more complex sample than uniform PCR products, longer oligonucleotide probes were chosen to avoid cross-reactivities and thus assure specificity. Therefore, the cantilevers were functionalized with the corresponding 18-mer thiol oligonucleotide probe (see Table 1) and an 18-mer reference

oligonucleotide (polyAC_long). The use of reference cantilevers is mandatory to eliminate temperature drift, unspecific binding and refractive index changes. Total RNA samples extracted from melanoma cell lines carrying wild type (T618A) or mutated (SK-Mel-37) BRAF sequences were injected at different concentrations, ranging from 5 to 300 ng/µl. The results of these experiments are shown in Fig. 3 a-d.

Four concentrations in the range of 5 to 300 ng/µl were measured, suggesting a lower limit of detection between 5 and 20 ng/µl total RNA. Best specificities were achieved at 100 and 20 ng/µl total RNA (Fig. 3b and c). As BRAF-mutated cancer cells still retain a normal copy of the wild type BRAF gene that can still be expressed, at variable levels, alongside the mutated form, using a wild type BRAF oligonucleotide as a reference instead of polyAC_long provides an important control. Using the corresponding 18-mer wild type oligonucleotide as reference, we observed a reduced response in the SK-Mel-37 signal (purple curve) as compared to the poly-AC differential signal (blue curve, Fig. 3e), consistent with a certain level of wild type BRAF expression in these cells (estimated at approximately 20% from Sanger sequencing plots, see supplementary figure 4). A positive signal (green curve) was observed using T618A RNA (BRAF wild type), as expected, due to binding to the wild type oligonucleotide (Fig. 3f). The increased noise observed during sample injection is likely due to the complexity of the total RNA samples. We further extended the RNA experiments to additional cell lines carrying either $BRAF^{V600E}$ or wild type BRAF sequences. Fig.4a and 4b show the results of experiments performed by injecting total RNA (at a concentration of 100 ng/µl) extracted from three different mutant cell lines (SK-Mel-37, Me246.M1 and Me275) and two different wild type cell lines (T618A and T1405B), respectively. The signals from the mutant cell lines differ substantially from those of the wild type ones. The stronger deflection observed for SK-Mel-37 compared to the other 2 mutant cell lines correlates with the higher BRAF levels expressed by these cells (see Methods). The results demonstrate the robustness of the assay to readily distinguish BRAF-mutated from BRAF wild type cell lines.

In summary, the experiments with melanoma samples demonstrate that mutant $BRAF^{V600E}$ can be identified in PCR products as well as in total RNA extracted from mutant cancer cell lines. The low concentration of total RNA required for the assay described here (20 ng/µl) indicates that this approach is applicable to clinical material. This could simplify and speed up the identification of tumours, reducing time to treatment. While we have focused here on the detection of $BRAF^{V600E}$ mutations in melanoma, the microcantilever approach can be extended to other relevant mutations recurring in other types of cancer (e.g. mutations in *KIT*, a receptor tyrosine kinase gene, in gastrointestinal stromal tumours and epidermal growth factor receptor mutations in lung cancer[27]). The proposed method has the following advantages: 1. samples do not have to be labelled or pre-amplified by PCR as total RNA samples can be utilised; 2. the technique is cost efficient and 3. due to the array format, the analysis can be paralleled, so that the presence of multiple mutations could be simultaneously interrogated, allowing a more detailed clinical prognosis, facilitating fast personalised medical diagnostics.

Methods:

Sensor preparation

Microcantilever arrays of eight silicon cantilevers (500 µm long, 100 µm wide and 1 µm thick) fabricated at IBM Research GmbH, Rüschlikon (Switzerland) were used in our experiments. For coating of microcantilever arrays with a receptor layer, we applied a previously described procedure[28]. Briefly, the arrays were cleaned in Piranha solution (30% H_2O_2:96% H_2SO_4 = 1:1, v/v) for 15 min, rinsed three times with water followed by isopropanol and dried in air. Thereafter, arrays were incubated for 30 min in 10 mM 2-[methoxypoly (ethyleneoxy)propyl] trimethoxysilane (7 ethylene glycol units, ABCR, Karlsruhe, Germany) solution in dry ethanol to reduce nonspecific binding to the lower silicon side. The array was then rinsed with isopropanol and dried in air. The

upper sides of cantilevers were subsequently coated with a 2 nm-layer of Ti followed by a 25 nm thick Au layer without breaking the vacuum. Deposition of metal layers was performed in an EVA 300 electron beam evaporator (Alliance Concept, Cran Gevrier, France) at an evaporation rate of 0.1 nm/s. Au-coated arrays were used immediately.

Probes

Oligonucleotides functionalized at the 5' end with a thiol group via a hexyl spacer were obtained from Microsynth GmbH (Balgach, Switzerland). The synthetic oligonucleotides used in this work are described in Table 1. Oligonucleotides were dissolved in 50 mM triethyl ammonium acetate buffer (TEAA, Fluka, Buchs, Switzerland), pH 7, at a concentration of 40 µM.

It is of paramount importance that measurements are performed in a differential fashion. External factors such as nonspecific interactions and thermal drift are cancelled out by calculating the differential response of a probe and a reference cantilever (in this study derivatised with a non-specific oligonucleotide of the same length as the probe sequence, or, in some experiments, with a wild type sequence). Eight microcapillaries (o.d. 250 µm; i.d. 150 µm; King Precision Glass, Inc., Claremont, CA) were filled with the appropriate oligonucleotide solution (probe or reference) to functionalise the cantilevers either with a probe layer or a reference layer. The cantilever array was then washed in 0.01x sodium-buffered saline citrate (SSC, Fluka) 1.5 mM NaCl and directly used for the analysis.

DNA and RNA sample preparation

Cell lines from melanoma metastases were established at LICR, Lausanne, except for SK-Mel-37 (a gift from Y. T. Chen, New York). SK-Mel-37, Me275, and Me246.M1 harbour mutated BRAF (cT1799A/V600E), while T618A and T1405B carry wild type BRAF, as assessed by Sanger sequencing. Total BRAF mRNA expression relative to T618A (set at 1) is 1.2, 0.9, 2.5, and 0.7 for Me275, Me246.M1, SK-Mel-37, and T1405B, respectively, as estimated by RNAseq[29] and/or PCR. Wild type

or mutated BRAF DNA sequences (621bp, spanning exon 13-18) were generated by PCR amplification of cDNA prepared from melanoma cell lines (T618Aand SK-Mel-37) as previously described[30]. Amplified products were concentrated by 2 rounds of ammonium acetate/ethanol precipitation and dissolved in TE buffer. Total RNA was extracted using Trizol reagent (Invitrogen) following manufacturer's instructions. RNA was further purified by ammonium acetate/ethanol precipitation and dissolved in DEPC-treated H_2O.

Prior to the experiments, the PCR amplified fragments were denatured at 96 °C for 10 min and cooled in an ice bath, forming single stranded segments along the DNA to enable hybridisation. Similarly, total RNA was heated to 70 °C for 5 min and cooled, denaturing the 3-dimensional structure of the RNA molecules to facilitate hybridisation.

Sensor instrument

The functionalized array was inserted into a liquid chamber (15 µl volume) and cantilever bending was measured using time multiplexed vertical-cavity surface-emitting lasers (VCSELs; wavelength 760 nm, Avalon Photonics, Zurich, Switzerland). The laser beam was deflected to a position sensitive detector (PSD, SiTek, Partille, Sweden). Data were acquired using a multifunctional data-acquisition board (National Instruments, Austin, TX) driven by LabView software. The software also controls the liquid handling system of the setup, the syringe pump (GENIE, Kent Scientific Corp, Torrington, CT), and a 10-position valve system (Rheodyne, Rohnert Park, CA). The entire setup was placed inside a temperature controlled box (Intertronic; Interdiscount, Switzerland), equilibrated through a fuzzy logic controller by the LabView software to keep the inside of the box at a temperature of 23 °C with an accuracy of ±0.02 °C.

Measurement and data analysis

Hybridisation experiments of PCR DNA fragments were conducted in 5x SSC and total RNA hybridisation was carried out in 0.01x SSC. A volume of 450 µl was injected in continuous flow at a

rate of 5 to 10 µl/min. Bimetallic response and mechanical properties of the cantilevers were assessed by applying 0.3 V to a Peltier element situated directly below the chamber for 70 s (thermal cycle). This resulted in a 2 °C pulse for deflection calibration. The average of all cantilevers together with the largest response was used to normalise the signal; provided the deflections did not differ by more than 10% in magnitude (usually 6 or more cantilevers satisfy this criterion). Normalised data from reference cantilevers were subtracted from the data of the probe cantilevers to obtain a differential signal. A baseline correction, required because drift behaviour of different cantilevers varies slightly, was applied, using a linear fit of data in the time interval beginning with buffer injection followed by DNA or RNA samples, respectively. The slope of the linear fit was subtracted from all differential signals.

References:

1. Ribas A. & Flaherty K.T. BRAF targeted therapy changes the treatment paradigm in melanoma. *Nat. Rev. Clin. Oncol.* **8**, 426-433 (2011).

2. Flaherty K.T. Dividing and conquering: controlling advanced melanoma by targeting oncogene-defined subsets. *Clin. Exp. Metastasis.* 29, 841-846 (2012).

3. Ravnan, M. C. & Matalka, M. S. Vemurafenib in Patients with *BRAF V600E* Mutation-Positive Advanced Melanoma. Clin. Ther. **34**, 1474-1486 (2012).

4. Flaherty, K. T. et al. Improved Survival with MEK Inhibition in BRAF-Mutated Melanoma. N. Engl. J. Med. **367**, 107-114 (2012).

5. Roskoski, R. RAF protein-serine/threonine kinases: Structure and regulation. *Biochem. Biophys. Res. Commun.* **399**, 313–317 (2010).

6. Gray-Schopfer V.C., da Rocha Dias S., Marais R. The role of B-RAF in melanoma. *Cancer Metastasis Rev.* **24**, 165-183 (2005).

7. Davies, H. et al. Mutations of the BRAF gene in human cancer. *Nature* **417**, 949-954 (2002).

8. Pratilas C. A., Xing F. & Solit D. B. Targeting Oncogenic BRAF in Human Cancer. *Therapeutic Kinase Inhibitors* **355**, 83-98 (2012).

9. Tiacci, E. et al. *BRAF* Mutations in Hairy-Cell Leukemia. *N. Engl. J. Med.* **364**, 2305-2315 (2011).

10. Halait, H. et al. Analytical Performance of a Real-time PCR-based Assay for V600 Mutations in the BRAF Gene, Used as the Companion Diagnostic Test for the Novel BRAF Inhibitor Vemurafenib in Metastatic Melanoma. *Diagn. Mol. Pathol.* **21**, 1-8 (2012).

11. Hinselwood, D. C., Abrahamsen, T. W. & Ekstrøm, P. O. BRAF mutation detection and identification by cycling temperature capillary electrophoresis. *Electrophoresis* **26**, 2553–2561 (2005).

12. Wu, C. C. et. al. Label-free biosensing of a gene mutation using a silicon nanowire field-effect transistor. *Biosens. Bioelectr.* **25**, 820–825 (2009).

13. Fang Z. & Kelley S. O. Direct Electrocatalytic mRNA Detection Using PNA-Nanowire Sensors. *Anal. Chem.* **81**, 612-617 (2009).

14. Fritz, J. et al. Translating Biomolecular Recognition into Nanomechanics. *Science* **288**, 316-318 (2000).

15. McKendry, R. et al. Multiple label-free biodetection and quantitative DNA-binding assays on a nanomechanical cantilever array. *Proc. Natl. Acad. Sci. USA* **99**, 9783–9788 (2002).

16. Biswal, S. L., Raorane, D., Chaiken, A., Birecki, H. & Majumdar, A. Nanomechanical Detection of DNA Melting on Microcantilever Surfaces. *Anal. Chem.* **78**, 7104-7109 (2006).

17. Mertens, J. Label-free detection of DNA hybridization based on hydration-induced tension in nucleic acid films. *Nature Nanotech.* **3**, 301-307 (2008).

18. Backmann, N. et al. A label-free immunosensor array using single-chain antibody fragments. *Proc. Natl. Acad. Sci. USA* **102**, 14587–14592 (2005).

19. Johansson, A., Blagoi, G. & Boisen A. Polymeric cantilever-based biosensors with integrated readout. *Appl. Phys. Lett.* **89**, DOI: 10.1063/1.2364843 173505 (2006).

20. Braun, T. et al. Conformational Change of Bacteriorhodopsin Quantitatively Monitored by Microcantilever Sensors. *Biophys. J.* **90**, 2970–2977 (2006).

21. Zhang, J. et al. Rapid and label-free nanomechanical detection of biomarker transcripts in human RNA. *Nature Nanotech.* **1**, 214-220 (2006).

22. Lang, H. P., Hegner, M. & Gerber, Ch. Cantilever array sensors. *Mater. Today* **8**, 30-36 (2005).

23. Yang, M., Yau, H. C. M. & Chan, H. L. Adsorption Kinetics and Ligand-Binding Properties of Thiol-Modified Double-Stranded DNA on a Gold Surface. *Langmuir* **14**, 6121-6129 (1998).

24. Nelson, B. P., Grimsrud, T. E., Liles, M. R., Goodman, R. M. & Corn, R. M. Surface Plasmon Resonance Imaging Measurements of DNA and RNA Hybridization Adsorption onto DNA Microarrays. *Anal. Chem.* **73**, 1–7 (2001).

25. Breslauer, K. J., Frank, R., Blocker, H. & Marky, L. A. Predicting DNA duplex stability from the base sequence. *Proc. Natl. Acad. Sci. USA* **83**, 3746–3750 (1986).

26. Barone, F., Cellai, L., Matzeu, M., Mazzei, F. & Pedone, F. DNA, RNA and hybrid RNA-DNA oligomers of identical sequence: structural and dynamic differences. *Biophys. Chem.* **86**, 37-47 (2000).

27. Stuart D. & Sellers W. R. Linking somatic genetic alterations in cancer to therapeutics. *Curr. Opin. Cell Biol.* **21**, 304-310 (2009).

28. Fritz, J. et al. Stress at the Solid-Liquid Interface of Self-Assembled Monolayers on Gold Investigated with a Nanomechanical Sensor. *Langmuir* **16**, 9694-9696 (2000).

29. Valsesia A. et al. Network-guided analysis of genes with altered somatic copy number and gene expression reveals pathways commonly perturbed in metastatic melanoma. *PLoS One* **6**, e18369. doi:10.1371/journal.pone.0018369 (2011).

30. Rimoldi, D. et al. Lack of BRAF Mutations in Uveal Melanoma. *Cancer Res.* **63**, 5712–5715 (2003).

Acknowledgments:

We acknowledge ongoing support from Michel Despont and Ute Drechsler (IBM Research GmbH, Rüschlikon, Switzerland) for providing cantilever arrays. We thank the National Center of Competence for Nanoscale Science (NCCR Nano), the Swiss Nano Institute (SNI), the NanoTera Program, the Cleven Foundation and the Swiss National Science Foundation for financial support. We thank Katja Muehlethaler for excellent technical assistance.

Author contributions:

F.H., D.R., C.G. conceived the study; F.H. and D.R., designed the experiments and interpreted the data; F.H. performed and analyzed the experiments; D. R. prepared DNA/RNA samples and cell lines; H.P.L. gold coated the cantilever arrays. F.H., D.R., H.P.L., C. G., N. B. wrote the manuscript. All authors discussed the results and commented on the manuscript.

Competing financial interests:

The authors declare that they have no competing financial interests.

Supplementary information accompanies this paper at www.nature.com/naturenanotechnology.

Reprints and permission information is available online at

http://npg.nature.com/reprintsandpermissions/.

Correspondence and requests for materials should be addressed to FH.

Figure legends:

Figure 1 Principle of microcantilever array functionalization and measurement. 1. The silicon array is coated with PEG-silane (brown ovals) to prevent non-specific adsorption to the lower cantilever side. 2. The array is coated with titanium as an adhesion layer and gold (in yellow) for thiol binding. 3. The cantilevers are either functionalized with a probe oligonucleotide (in red) or a non-specific reference oligonucleotide (in light blue). 4. Injection of the target (a) DNA or (b) RNA containing the complementary (matching) sequence (depicted in green) to the probe oligonucleotide (red). Non-related sequences are displayed in black. Upon hybridisation only the probe cantilever is bending giving rise to a differential deflection Δx. No binding occurs on the reference cantilever.

Figure 2 Compressive surface stress from hybridisation experiments with PCR- amplified BRAF sequences. (**a**) Differential surface stress measured after injection of different ratios of wild type to mutant DNA, as indicated in the box. Differential signals between probe (derivatised with V600E_short) and reference cantilevers (derivatised with polyAC_short) are shown. Fluctuations after sample injection are due to mixing of buffer, DNA solution and switching of valves, but do not influence the later equilibrium cantilever deflection before performing a washing step with 5x SSC (sodium-buffered saline citrate). The differently coloured bars at the bottom indicate the duration of

injection and solution being injected (light grey: buffer, orange: DNA sample). The dashed vertical lines separate different injections. (**b**) Langmuir isotherm with an $R^2 = 0.97$, indicating a reliable fit with the data. The experiments show that the 13-mer BRAF sequence can be detected in a larger DNA fragment at various concentrations.

Figure 3 Detection of mutated versus wild type BRAF in total RNA samples. In (a to d), total RNA samples from T618A (wild type, black) and SK-Mel-37 ($BRAF^{V600E}$, red) cells were injected at the indicated concentrations. The bars at the bottom of the graphs indicate the solution being injected and different injection periods are marked by dashed vertical lines: buffer (light grey), total RNA from T618A (dark grey) and SK-Mel-37 cell lines (light red). Differential signals between probe (V600E_long functionalized) and reference cantilevers (polyAC_long functionalized) are shown. At the highest concentration measured of 300 ng/µl (a) mutant and wild type sequences cannot be clearly distinguished indicating increased cross hybridisation by the wild type sequence. We are able to distinguish reliably mutant BRAF from wild type BRAF at concentrations of 100 and 20 ng/µl (b and c). A signal of 4 nm at a concentration as low as 5 ng/µl total RNA was observed (d) indicating a limit of detection between 5 and 20 ng/µl. Experiments shown in (e) using total RNA from SK-Mel-37 cells and poly-AC (blue dots) or wild type (purple dots) oligonucleotides as references, respectively (the light grey bars indicate buffer and the orange bar SK-Mel-37 sample injection). In the lower graph (f) the response of total RNA from wild type T618A is shown using a wild type oligonucleotide reference (green dots). Here we show that the assay can distinguish between wild type and mutant BRAF mRNA in a complex background of non-related sequences.

Figure 4 Analysis of RNA samples from different tumour and wild type cells. Differential signals between probe (V600E_long functionalized) and reference cantilevers (polyAC_long functionalized)

are shown. (a) Total RNA from mutant $BRAF^{V600E}$ cell lines shows consistently a higher signal than RNA from wild type samples (b). After equilibrating the microcantilever array with 0.01x SSC buffer (light grey bar), 450 µl of total RNA (100 ng/µl) was injected (orange bar). The dashed vertical lines indicate the different injection periods. This experiment shows that the assay does not depend on the cell lines used; different BRAF mutant cell lines can be distinguished from wild type cell lines.

Probe	Sequence	Use
V600E_short	5'-CTACAG**A**GAAATC-3'	Detection of 621bp mutated cDNA PCR product (see Figure 2).
polyAC_short	5'-ACACACACACACA-3'	Reference for detection of 621bp mutated cDNA PCR product (see Figure 2).
V600E_long	5'-GAGATTTC**T**CTGTAGCTA-3'	Detection of $BRAF^{V600E}$ in total RNA (see Figures 3 and 4).
polyAC_long	5'- ACACACACACACACACAC-3'	Reference for BRAF RNA detection (see Figures 3 and 4)
wt_long	5'-GAGATTTC**A**CTGTAGCTA-3'	Additional reference in $BRAF^{V600E}$ detection (see Figures 3 e and f).

Table 1. Oligonucleotide probes used in the study. The nucleotides important for the detection (corresponding to the cT1799A/V600E mutation) are labelled in red. Note that V600E short and long, both designed to detect the mutation, were chosen from opposite DNA strands (hence the different, but complementary, sequence).

1. PEG silane

2. 20nm Au/2nm Ti coating

3. Probe oligonucleotide

Reference oligonucleotides

4. Hybridisation

a. DNA

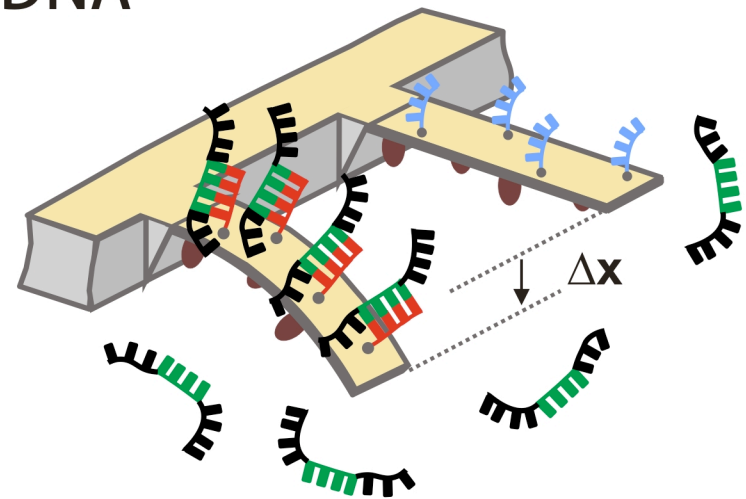

b. RNA

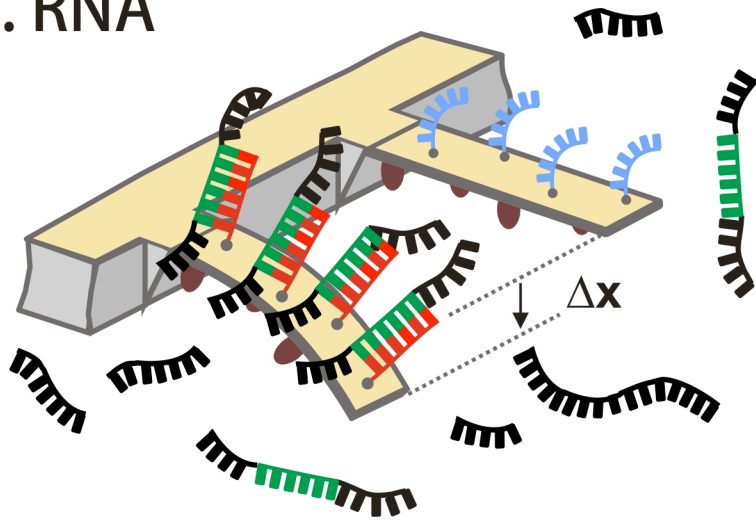

DNA target sequence

RNA target sequence

unrelated sequences

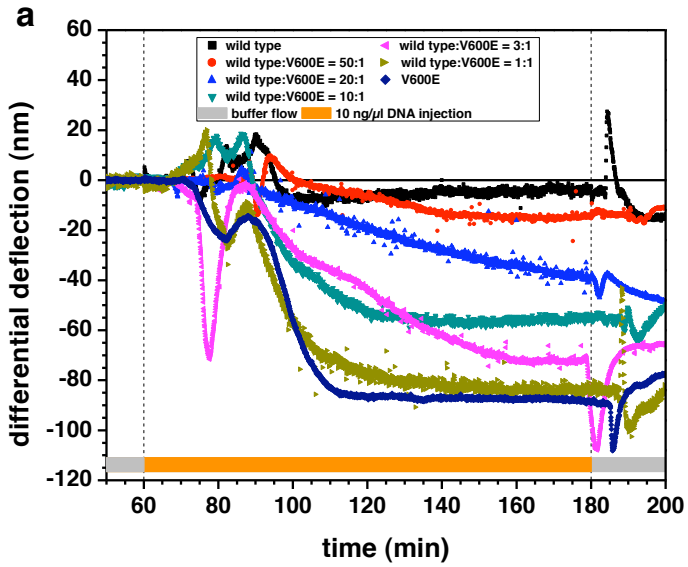
a
wild type
wild type:V600E = 50:1
wild type:V600E = 20:1
wild type:V600E = 10:1
wild type:V600E = 3:1
wild type:V600E = 1:1
V600E
buffer flow
10 ng/µl DNA injection
differential deflection (nm)
time (min)

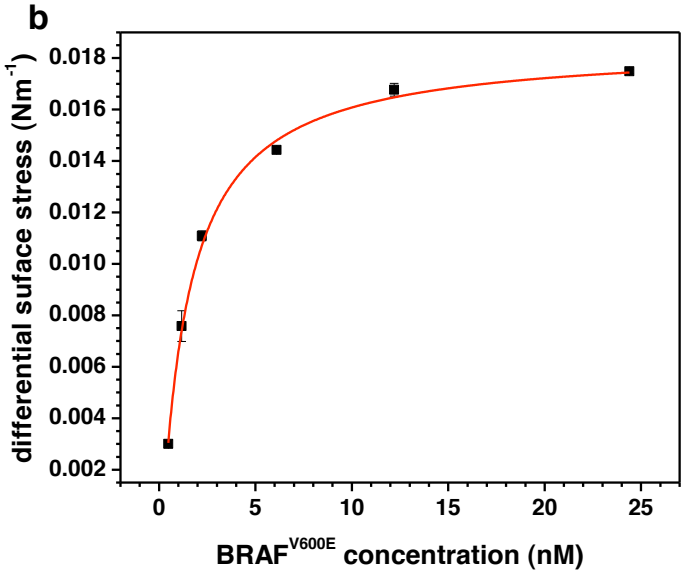
b
differential suface stress (Nm-1)
BRAFV600E concentration (nM)

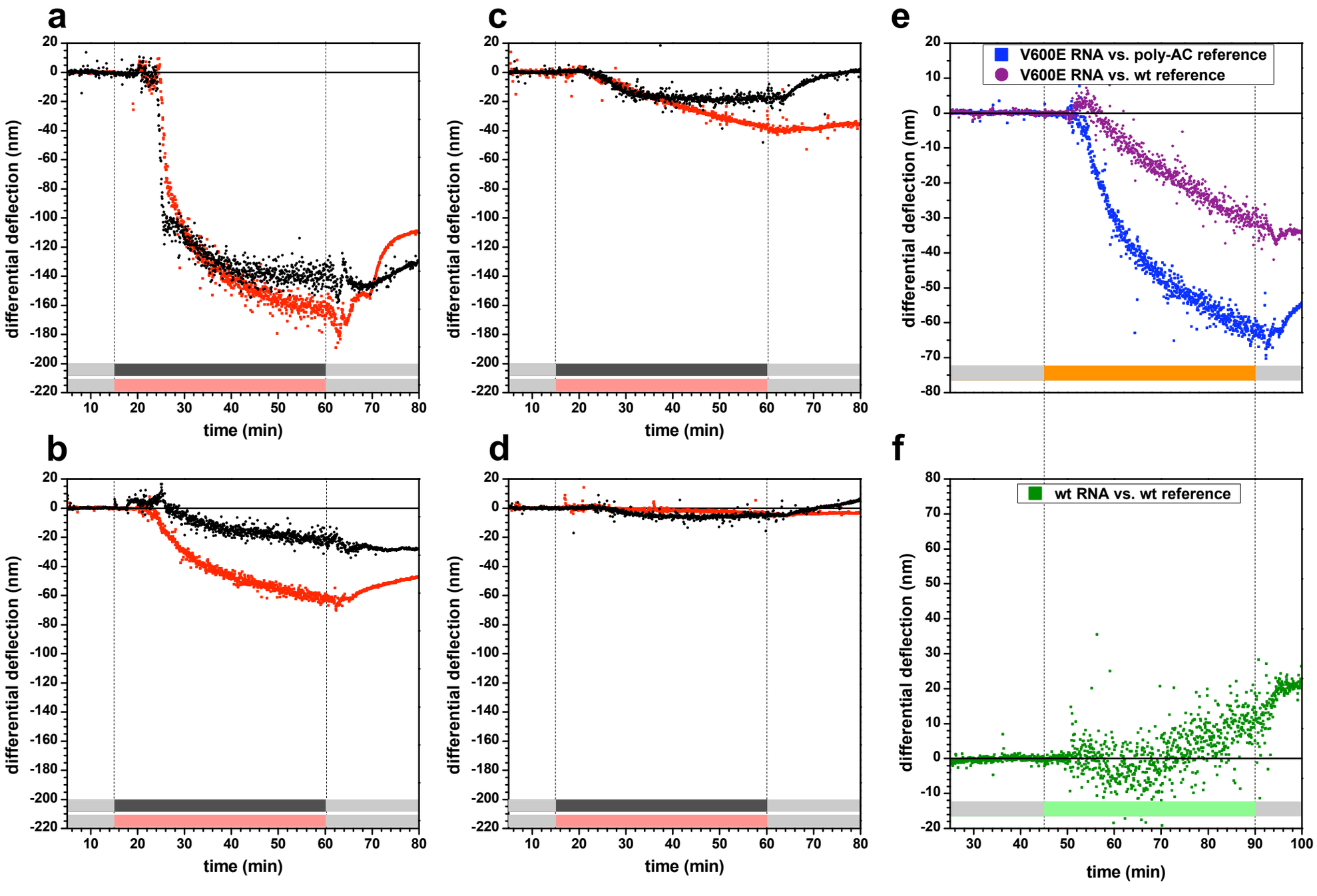
a
b
c
d
e
f
differential deflection (nm)
time (min)
V600E RNA vs. poly-AC reference
V600E RNA vs. wt reference
wt RNA vs. wt reference

a

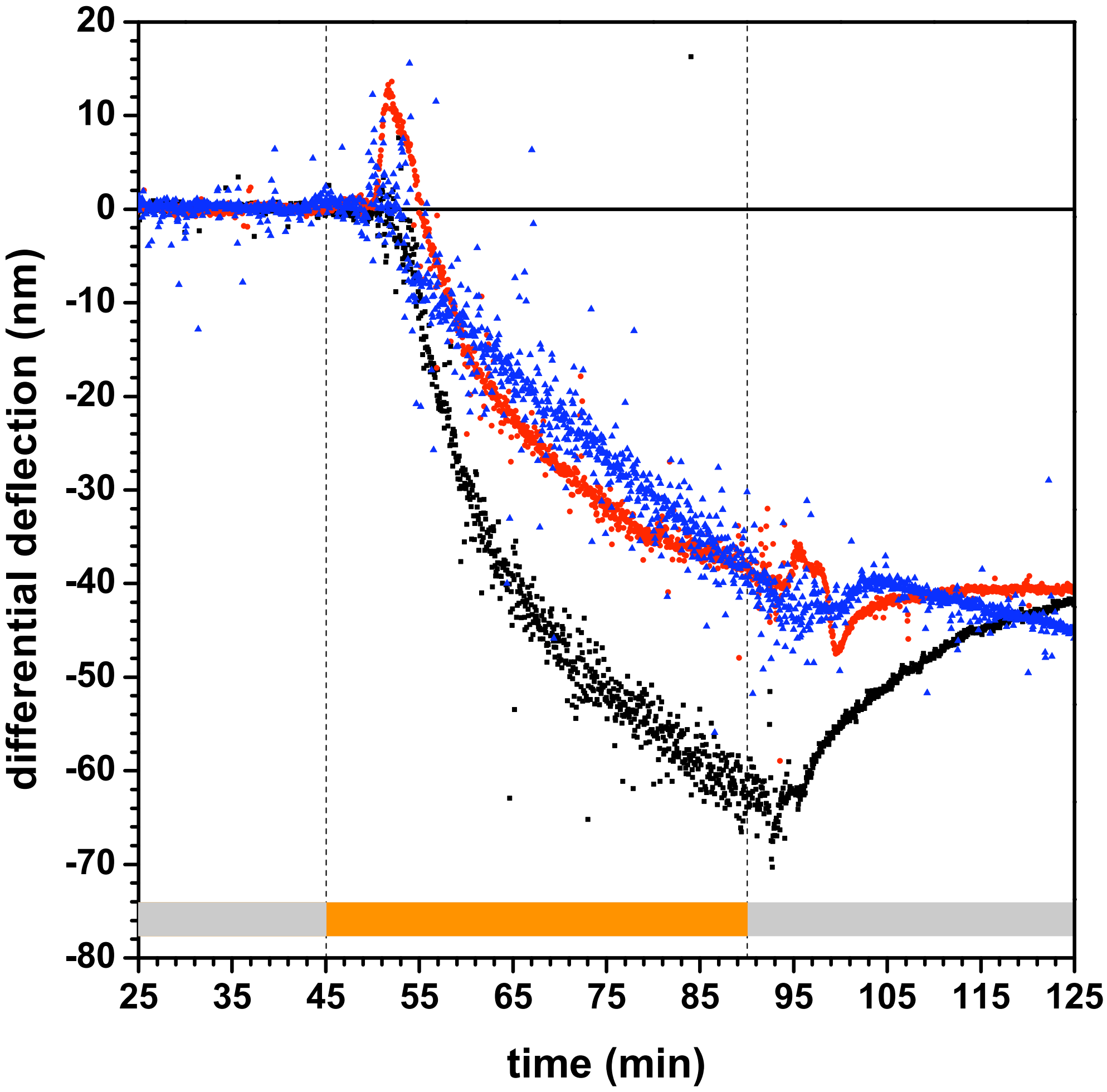
20
10
0
-10
-20
-30
-40
-50
-60
-70
-80
differential deflection (nm)
25
35
45
55
65
75
85
95
105
115
125
time (min)

b

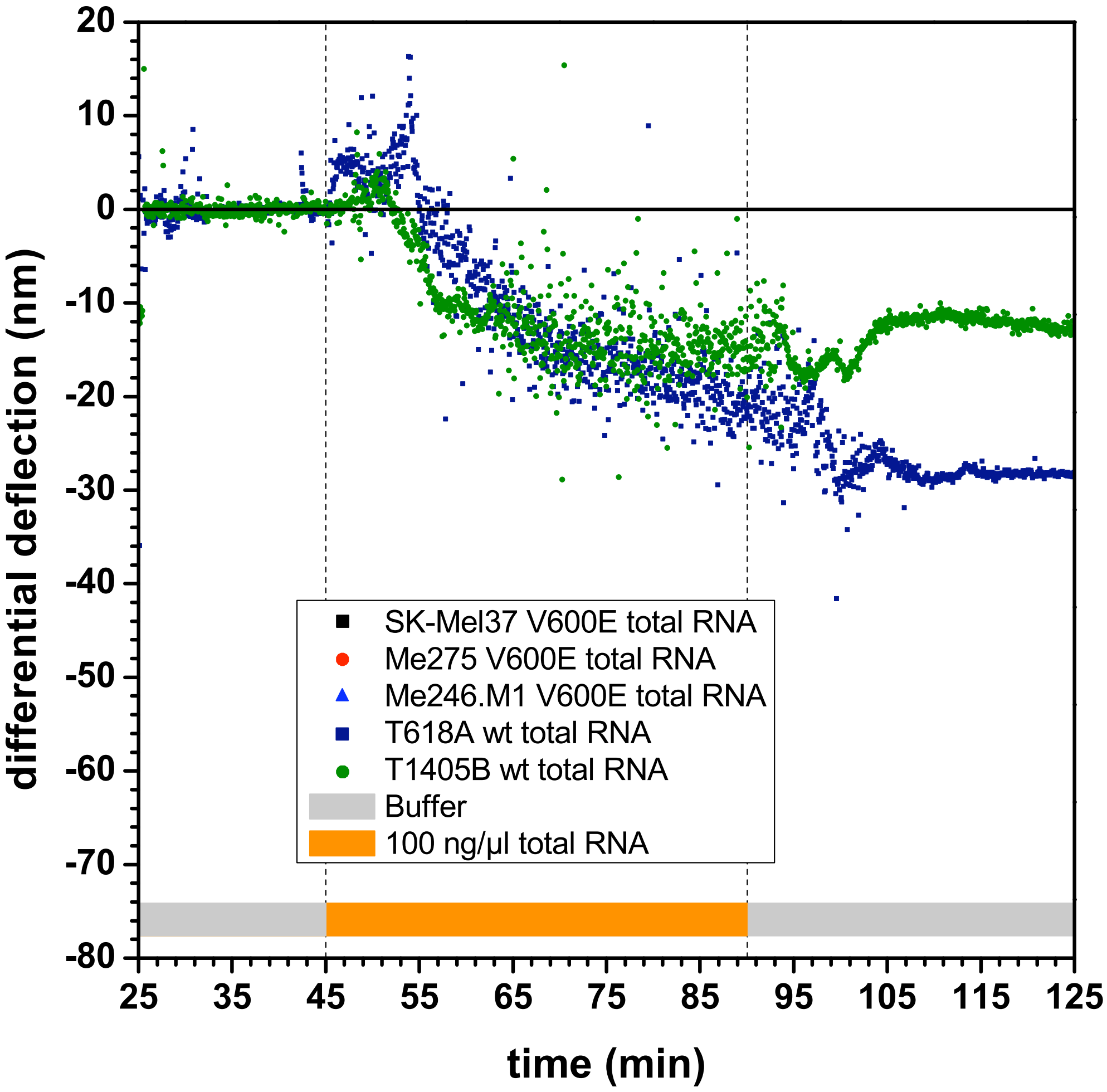
20
10
0
-10
-20
-30
-40
-50
-60
-70
-80
differential deflection (nm)
SK-Mel37 V600E total RNA
Me275 V600E total RNA
Me246.M1 V600E total RNA
T618A wt total RNA
T1405B wt total RNA
Buffer
100 ng/µl total RNA
25
35
45
55
65
75
85
95
105
115
125
time (min)

Title: Direct Detection of a BRAF Mutation in total RNA from Melanoma Cells

Authors:

F. Huber, H. P. Lang, N. Backmann, D. Rimoldi and Ch. Gerber

Supplementary Information

We performed preliminary tests to optimise the adsorption of V600E_short thiol oligonucleotide probes onto a gold-coated cantilever surface. To this end, one half of a microcantilever array (Supplementary Figure 1a) previously coated with titanium and gold was functionalised with the polyAC_short thiol oligonucleotide to passivate the gold surface and serve as reference, thus leaving 4 unfunctionalised cantilevers (probe cantilevers) for DNA adsorption tests (Supplementary Figure 1b).

Previous studies[1,2] have shown that concentrations of DNA solutions in the range of 1-10 µM are sufficient to saturate the gold surface. Here, we studied the sensitivity of the device to detect DNA oligonucleotide adsorption over 3 orders of magnitude, extending the measurements to lower as well as higher concentrations. We thus injected various concentrations (10nM to 40µM) of the thiol oligonucleotide V600E_short and measured the deflection signal (Supplementary Figure 2). The extracted dissociation constant $K_D = 3.5x10^{-5}$ M^{-1} characterising the adsorption process of V600E_short on gold corresponds to a free energy change of $\Delta G = 30.6$ $kJmol^{-1}$ and is in agreement with previous measurements performed with piezoresistive microcantilevers or the quartz crystal microbalance method[3,4].

We were first investigating the surface coverage of thiol oligonucleotides and secondly performed proof of concept hybridisation experiments with complementary oligonucleotides and PCR amplified DNA. These experiments allowed optimising the conditions for directly detecting the mutation in total RNA. With the experiments using urea we verified reusability of the sensor for subsequent experiments.

We used cantilever arrays derivatised as described above (with 4 cantilevers coated with V600E_short and 4 with the polyAC_short oligonucleotide, both thiol-modified) in hybridisation experiments using a V600E_short-complementary oligonucleotide, i.e. 5'-GATTTCTCTGTAG-3' (referred to as $BRAF^{V600E}$, mutation in red), as test sample. In Supplementary Figure 3 the response observed in 5 subsequent injections of 500nM complementary $BRAF^{V600E}$ oligonucleotide is shown, interrupted by urea/dehybridisation and buffer/washing steps to regenerate the microcantilever array.

Within 10 min after injection of the sample solution, a signal of 200nm developed indicating hybridisation. The subsequent urea denaturing step showed a large negative dip due to the abrupt change in the refractive index switching from 30% urea to the 5xSSC buffer solution used in the hybridisation step. Shortly after injection of hybridisation buffer, the signal re-equilibrated to zero. Repeating this cycle five times resulted in an average differential deflection of 178 ±19 nm corresponding to a surface stress change of -0.035 ±0.0046 N/m, demonstrating high reproducibility of $BRAF^{V600E}$ hybridisation measured with microcantilevers.

Sanger Sequencing (supplementary Figure 4) reveals a mixed expression of both the mutated and, at a lower level, of the wild type BRAF gene copies in SK-Mel-37 cells.

References

1. McKendry, R. et al. Multiple label-free biodetection and quantitative DNA-binding assays on a nanomechanical cantilever array. *Proc. Natl. Acad. Sci. USA* **99**, 9783–9788 (2002).

2. Steel, A. B., Levicky, R. L., Herne, T. M. & Tarlov, M. J. Immobilization of Nucleic Acids at Solid Surfaces: Effect of Oligonucleotide Length on Layer Assembly. *Biophys. J.* **79,** 975–981 (2000).

3. Marie, R. et al. Immobilisation of DNA to polymerised SU-8 photoresist. *Biosens. Bioelectron.* **21** 1327–1332 (2006).

4. Yang, M., Yau, H. C. M. & Chan, H. L. Adsorption Kinetics and Ligand-Binding Properties of Thiol-Modified Double-Stranded DNA on a Gold Surface. *Langmuir* **14**, 6121-6129 (1998).

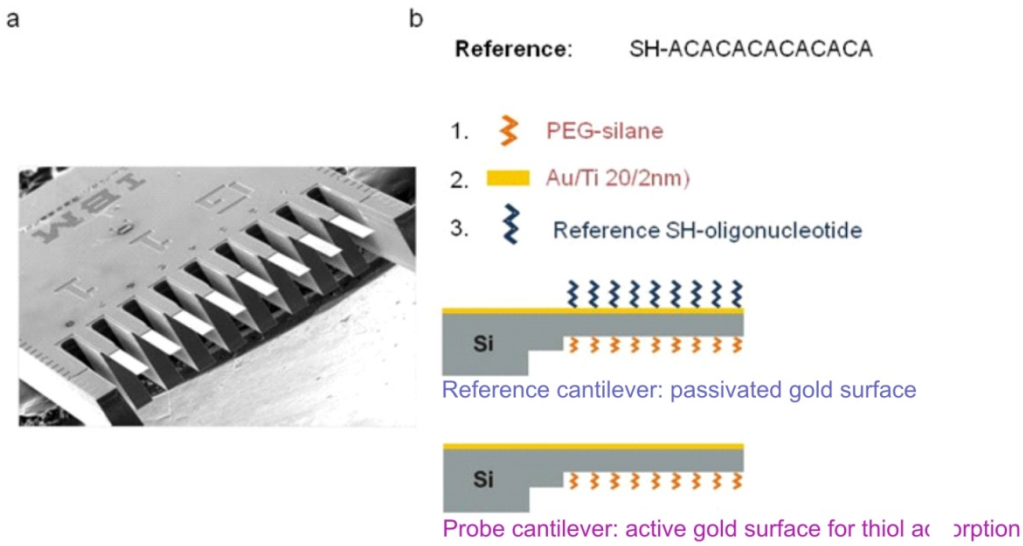

Supplementary Figure 1 Schematics of microcantilever array functionalisation to test adsorption of the oligonucleotide probe. (a) picture of a microcantilever array. (b) shows the thiol oligonucleotide polyAC_short and the different preparation steps: 1. the silicon array is coated with PEG-silane to prevent a non-specific adsorption of DNA on the lower cantilever side, 2. the array is coated with titanium and gold and 3. the reference cantilevers are functionalised with polyAC_short to passivate the gold surface. We now have prepared an array of microcantilevers with an active gold surface ready for the thiol-oligonucleotide adsorption as well as reference cantilevers with a passivated gold surface.

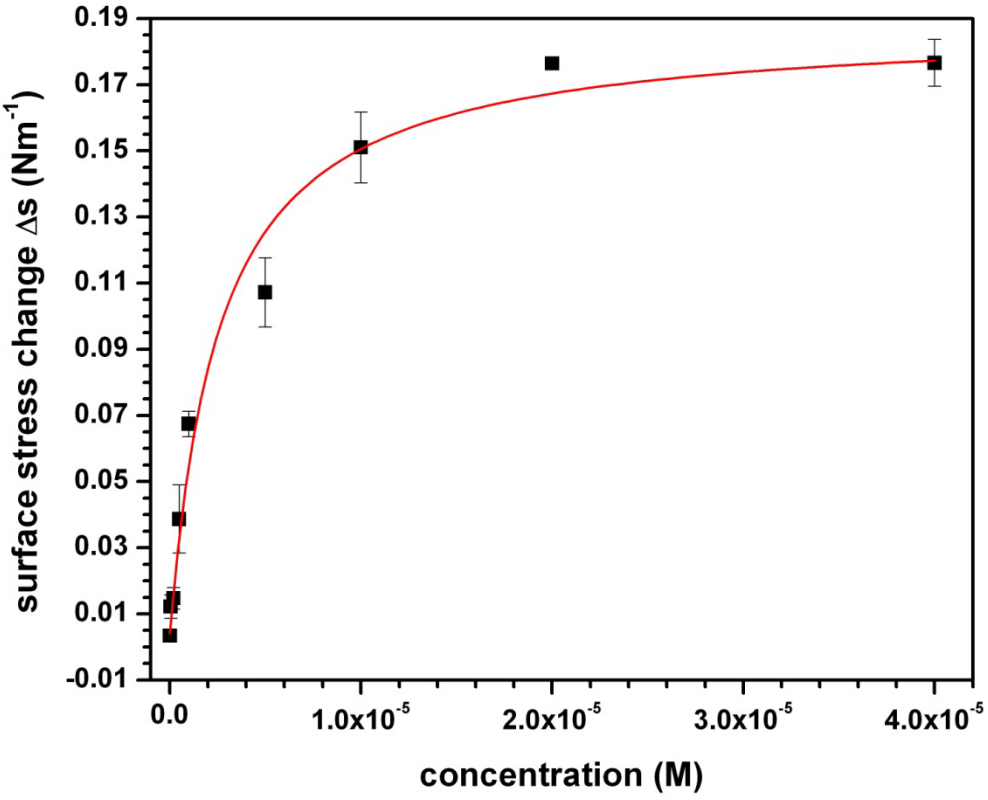

Supplementary Figure 2 Adsorption of thiol oligonucleotide V600E_short to gold coated microcantilevers. The equilibrium surface stress (black filled squares) generated during adsorption of oligonucleotides is plotted against various oligonucleotide concentrations (10nM, 50nM, 200nM, 500nM, 1µM, 5µM, 10µM, 20µM, 40µM). The red solid line shows the Langmuir isotherm (R^2=0.98) from which the maximum surface stress s_{max} = 0.18 ±0.01 Nm^{-1} and the dissociation constant K_D = (2.58 ±0.5) x 10^{-6} M are derived.

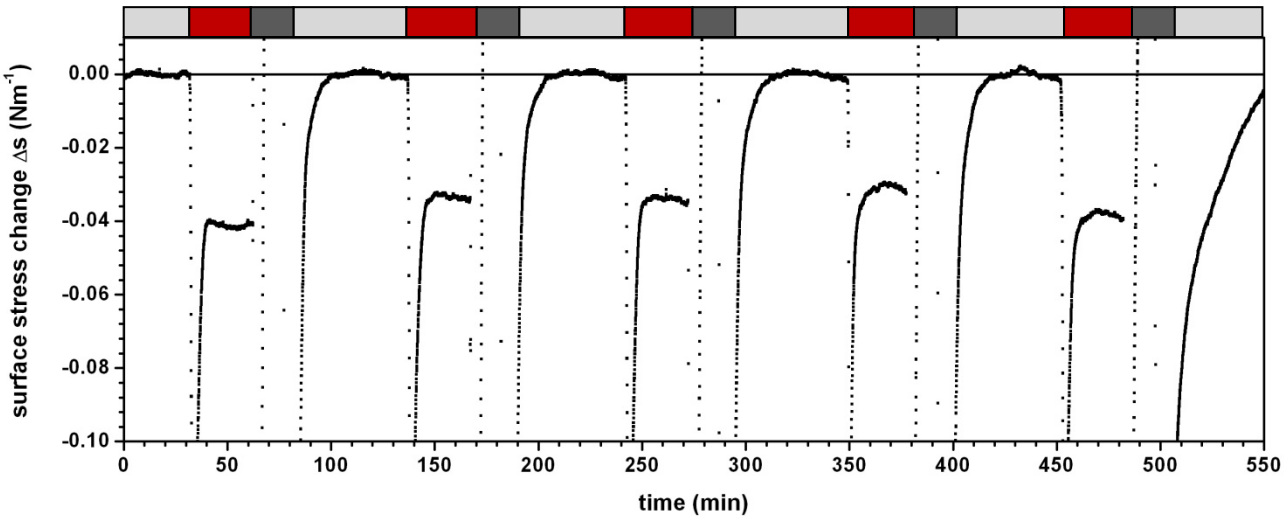

Supplementary Figure 3 Repeated hybridisation cycles of complementary BRAF^{V600E} oligonucleotide. Surface stress changes are plotted versus time. We observe a compressive surface stress change upon injection of BRAF^{V600E}. The bar on top of the graph shows the injection cycle: light grey, washing with hybridisation buffer; red, injection of 500nM complementary mutant BRAF^{V600E} dark grey, flushing with 30% urea solution.

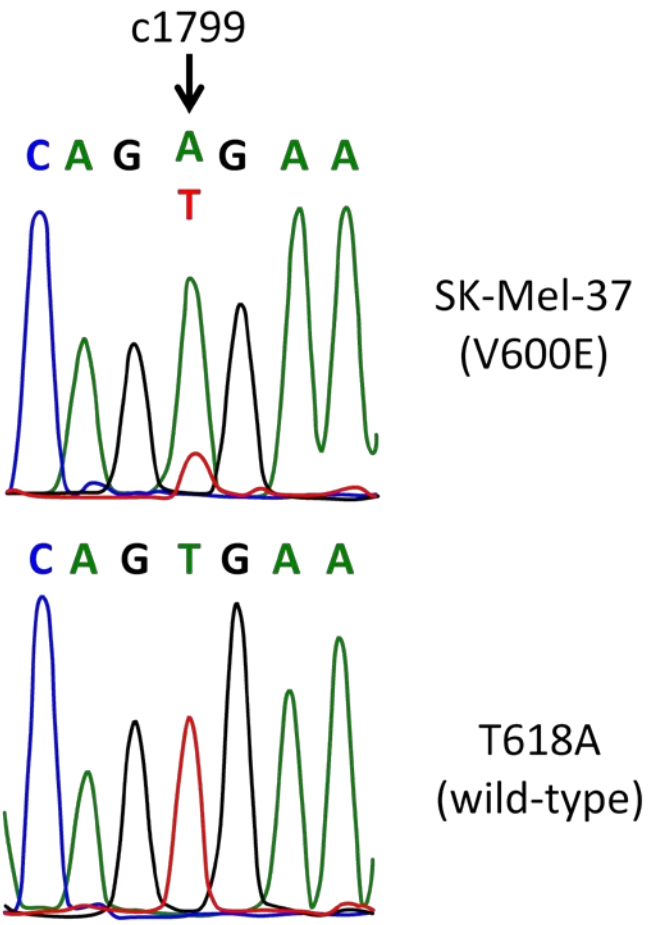

Supplementary Figure 4 Detection of BRAF cT1799A/V600E mutation in melanoma cells by Sanger sequencing. Chromatograms show nucleotide sequence around c1799 obtained from sequencing of BRAF cDNA from SK-Mel-37 and T618A melanoma cells. Mixed expression of wild type and mutant BRAF in SK-Mel-37 cells is indicated by the overlapping signal at nucleotide c1799 (T/red, wild type; A/green, mutant gene).